Electronic Supplementary Material (ESI) for Journal of Materials Chemistry A.

Supporting Information for

High-Performance Protonic Ceramic Fuel Cell Cathode using Protophilic Mixed Ion and Electron Conducting Material

Dingyue Hu[1], Junyoung Kim[1], Hongjun Niu[1], Luke M. Daniels[1], Troy D. Manning[1], Ruiyong Chen[1], Bowen Liu[1], Richard Feetham[1], John B. Claridge[1], Matthew J. Rosseinsky[1].
[1] Department of Chemistry, Materials Innovation Factory, University of Liverpool, 51 Oxford Street, Liverpool, L7 3NY

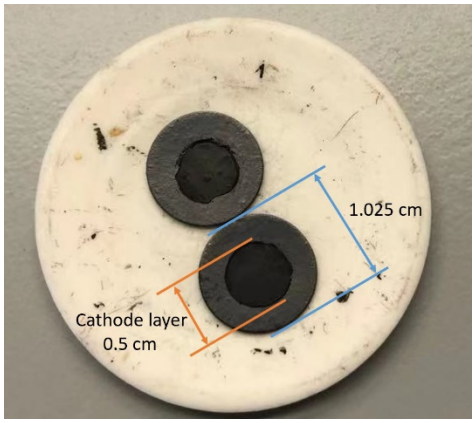

Figure S1. The photo of NiO-BZCYYb anode-supported BSCFW single cell after firing at 950 °C. The diameter of the single cell is 1.025 cm and the diameter of the cathode layer is 0.5 cm.

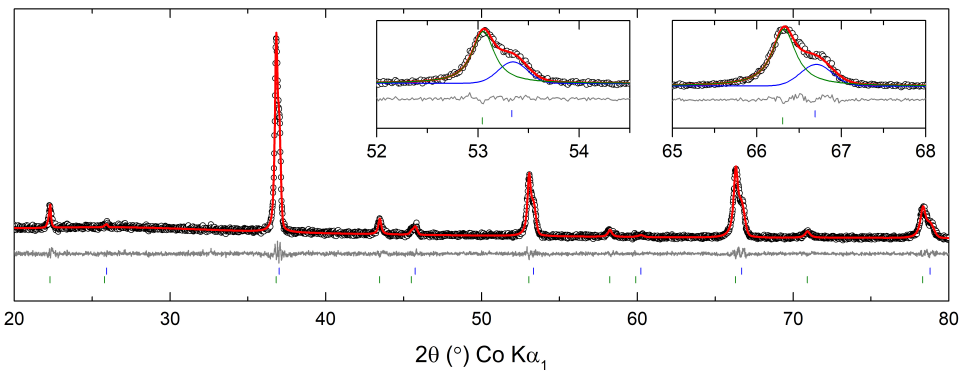

Figure S2. Pawley fit performed on data collected from BSCFW powder using a Co $K\alpha_1$ source Panalytical instrument showing how peaks from the SP and DP phases can be distinguished. Black circles (data), red line (calculated profile), grey line (difference profile), and insets show peak contributions from DP (green) and SP (blue).

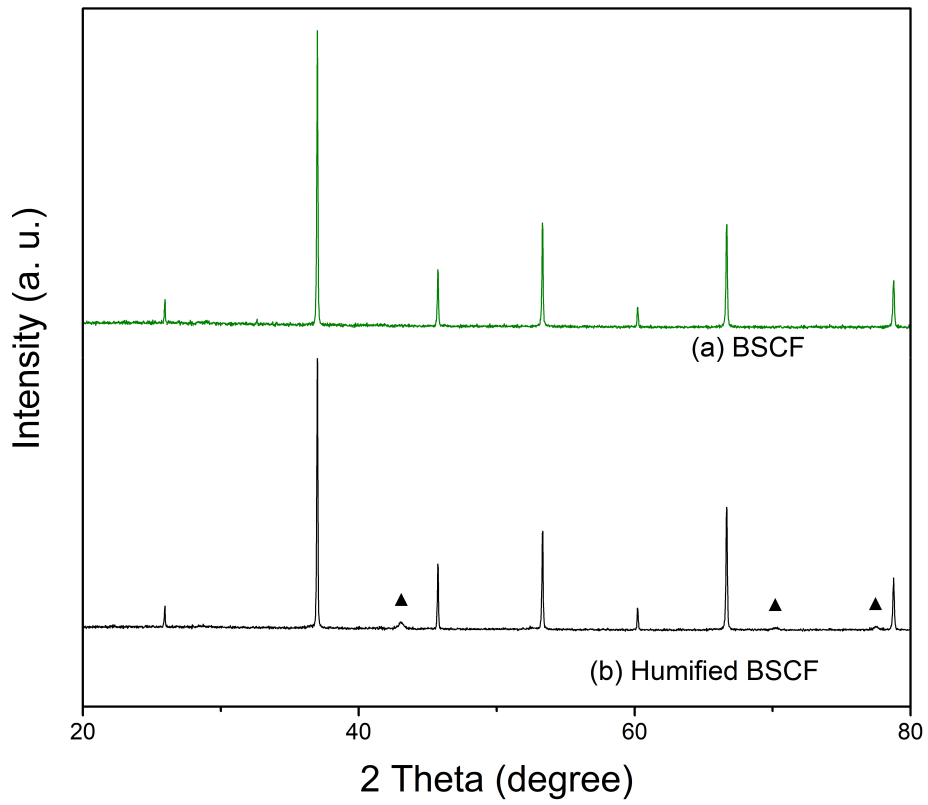

Figure S3. XRD patterns of BSCF (a) before and (b) after hydration. For hydration, BSCF powder was heated to 900 °C and then held at 300 °C under 3 vol% H_2O-containing air for 1h. Triangle symbols (▲) indicate the formation of a Co_3O_4 secondary phase.

Table S1 The calculated B-site cation occupancy and average cation radii for BSCFW based on the combined refinement results using I11 and neutron diffractions.[1] (Note the ionic radii of B-site cations (Co^{2+}: 74.5 pm, Co^{3+}: 61 pm, Fe^{3+}: 64.5 pm, W^{6+}: 60 pm) used in the calculation are all quoted from R.D Shannon's study[2]).

DP phase $BaSrCo_{0.847(12)}Fe_{0.260(22)}W_{0.891(17)}O_6$				
Co^{2+} at.%	Fe^{3+} at.%	W^{6+} at.%	Occupancy sum	B-site cation average radius (pm)
0.847(12)	0.260(22)	0.891(17)	2.00(5)	66.73

SP phase	$Ba_{0.5}Sr_{0.5}Co_{0.589(10)}Fe_{0.354(9)}W_{0.056(3)}O_{2.304(21)}$			
Co^{3+} at.%	Fe^{3+} at.%	W^{6+} at.%	Occupancy sum	B-site cation average radius (pm)
0.589(10)	0.354(9)	0.056(3)	1.00(2)	62.18

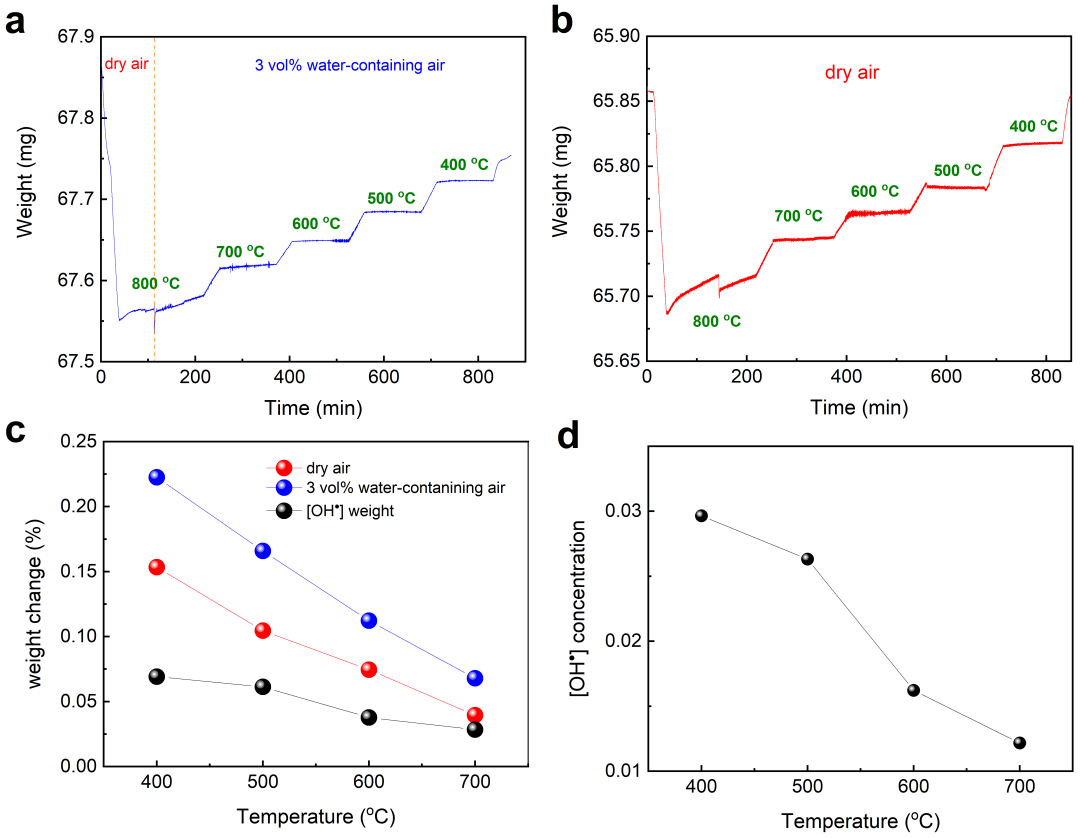

Figure S4. BSCFW measured by thermogravimetric analysis (TGA) from 800 °C to 400 °C under 3 vol% H_2O-containing air (a) and dry air (b). The mass of the BSCFW powder used for TGA measurement in wet air and dry air are 67.87234 mg and 65.85087 mg, respectively. (c) Weight change (compared to the weight of BSCFW under dry air at 800 °C) under dry air (red line) and wet air (blue line) at various temperatures (400 °C, 500 °C, 600 °C and 700 °C) and the approximate proton weight (%) in BSCFW sample. (d) proton concentration as a function of temperature. Proton concentrations are given in units of [(OH mol concentration)/(mol concentration of lattice oxygen for dried-BSCFW)]. The lattice oxygen (3-δ) of dried-BSCFW at 400 °C, 500 °C, 600 °C and 700 °C are 2.773(1), 2.765(1), 2.760(1)[1], and 2.754(1) respectively based on the TGA data presented here and the diffraction refinement results of BSCFW reported in *Nat. Energy*, 2017, **2**, 16214.

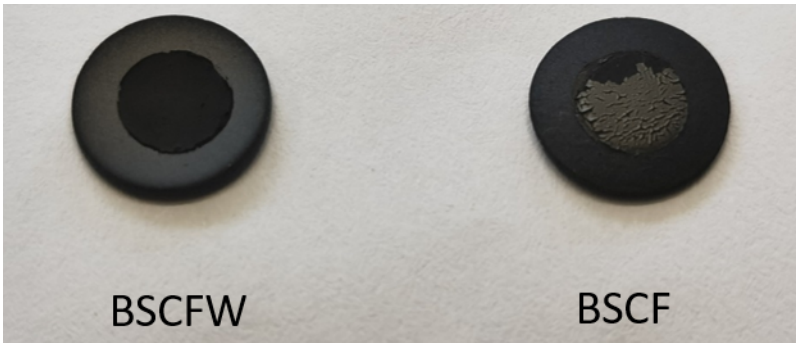

Figure S5. Photograph of symmetrical cells of (left) BSCFW|BZCYYb|BSCFW and (right) BSCF|BZCYYb|BSCF. The delamination of BSCF is clearly observed.

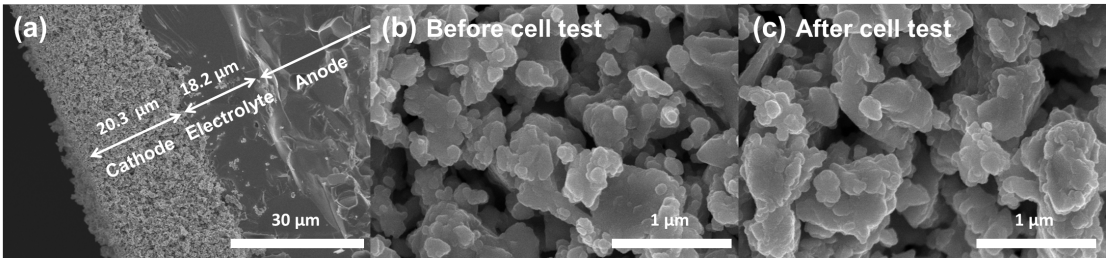

Figure S6. (a) Cross-sectional SEM image of BSCFW/BZCYYb/NiO-BZCYYb cell. SEM images of porous BSCFW cathode (b) before and (c) after single cell tests.

Figure S6 shows the microstructure of the BSCFW cathode and single cell (BSCFW|BZCYYb|NiO-BZCYYb) by SEM image. The BSCFW cathode has a highly porous morphology that ensures high surface area and good gas diffusion. As shown in **Figure S6a**, the dense BZCYYb electrolyte and the porous BSCFW cathode (ca. 20.3 μm thick) are successfully fabricated. The BSCFW cathodes adhere well onto the BZCYYb electrolyte without any cracks or delamination, which is expected to enhance the mechanical compatibility and the long-term stability of the cathode-electrolyte interface. As can be seen in **Figure S6b** and **c**, there is no observable difference of cathode microstructure before and after the single cell test, indicating that the BSCFW cathode shows a good microstructural durability under the practical single cell test environment.

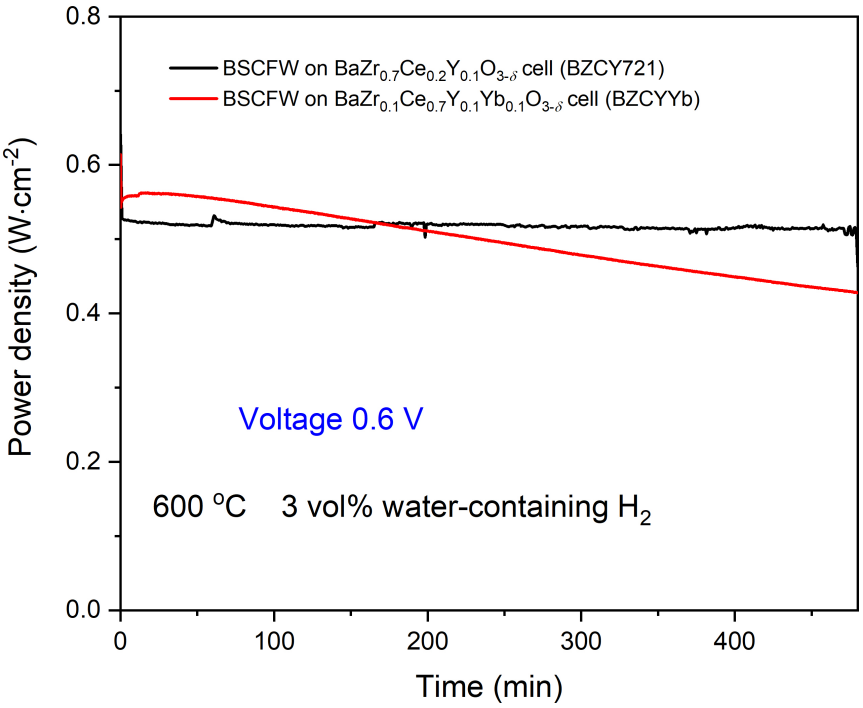

Figure S7. Power density plotted *versus* time of BSCFW|BZCY721|NiO-BZCY (black line) and BSCFW|BZCYYb|NiO-BZCYYb (red line) single cell held at 600 °C using 3 vol% water-containing H_2 as fuel for 8 h. This operational stability test applied a constant voltage (0.6 V) on the single cell and collected the current every 5 min. The degradation rate of the power density of BSCFW|BZCY721|NiO-BZCY single cell is $2.2(1) \times 10^{-5}$ W cm^{-2} min^{-1}, while the degradation value of BSCFW|BZCYYb|NiO-BZCYYb cell is $3.0(2) \times 10^{-4}$ W cm^{-2} min^{-1}.

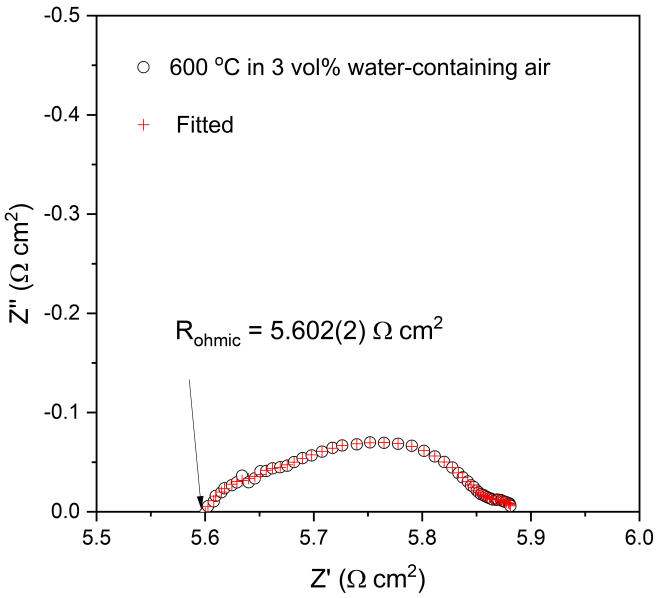

Figure S8. The original impedance data of a BSCFW|BZCYYb|BSCFW symmetrical cell held at 600 °C in 3 vol% water-containing air for 5 h (achieved an equilibrium state). The ohmic resistance is the contribution from the electrolyte. The R_{ohmic} of BZCYYb is 5.602(2) Ω cm^2, and the conductivity of BZCYYb at 600 °C in wet air is calculated as L/R_{ohmic} = 0.196/5.602 = 0.035 S cm^{-1}, where L is the thickness of the BZCYYb pellet (0.196 cm). This result is close to the value reported for BZCYYb (~0.03 S cm^{-1}).[3, 4]

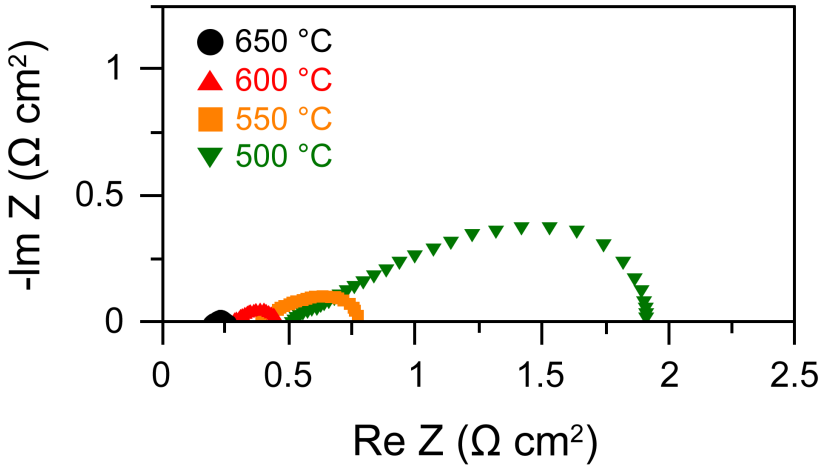

Figure S9. Impedance data of BSCFW single cell (**Figure 5d**) in full-scale.

Table S2. Comparison of the decay rate of the power output for representative PCFC cells reported recently.

Cell composition	Decay rate (W cm^2 min^{-1})	Ref.
KSCN-BZCY	~3.2 ×10^{-5}	ChemSusChem, 2021, 14, 3876-3886
NBSCF−NDC	~3×10^{-6}	ACS Appl. Mater. Interfaces, 2018, 11, 457-468
3-SEFC0.5-BZCY	~8.3×10^{-6}	ChemSusChem, 2020, 13, 4994-5003

LSCF-BZCY	~3.3×10^{-5}	J. Power Sources, 2015, 278, 320-324
BSCFW-BZCY	$2.2(1) \times 10^{-5}$	This work
BSCFW-BZCYYb	$3.0(2) \times 10^{-4}$	This work

Additional references

1. J. F. Shin, W. Xu, M. Zanella, K. Dawson, S. N. Savvin, J. B. Claridge and M. J. Rosseinsky, *Nat. Energy*, 2017, **2**, 16214.
2. R. D. Shannon, *Acta Crystallographica Section A*, 1976, **32**.
3. L. Yang, S. Wang, K. Blinn, M. Liu, Z. Liu, Z. Cheng and M. Liu, *Science*, 2009, **326**, 126-129.
4. N. T. Q. Nguyen and H. H. Yoon, *J. Power Sources*, 2013, **231**, 213-218.